Research Article Vol. 2, No. 4 / April 2015 / Optica 357

Performance metrics and design considerations for a free-space optical orbital-angular-momentum–multiplexed communication link

Guodong Xie,[1,*] Long Li,[1] Yongxiong Ren,[1] Hao Huang,[1] Yan Yan,[1] Nisar Ahmed,[1] Zhe Zhao,[1] Martin P. J. Lavery,[2] Nima Ashrafi,[3] Solyman Ashrafi,[3] Robert Bock,[4] Moshe Tur,[5] Andreas F. Molisch,[1] and Alan E. Willner[1,6]

[1]Department of Electrical Engineering, University of Southern California, Los Angeles, California 90089, USA
[2]School of Physics and Astronomy, University of Glasgow, Glasgow, G12 8QQ, UK
[3]NxGen Partners, Dallas, Texas 75219, USA
[4]R-DEX Systems, Marietta, Georgia 30068, USA
[5]School of Electrical Engineering, Tel Aviv University, Ramat Aviv 69978, Israel
[6]e-mail: willner@usc.edu
*Corresponding author: guodongx@usc.edu

Received 19 October 2014; revised 11 February 2015; accepted 10 March 2015 (Doc. ID 225215); published 8 April 2015

The capacity of free-space optical (FSO) communication links could potentially be increased by the simultaneous transmission of multiple orbital angular momentum (OAM) beams. For such an OAM multiplexing approach, one requires the collection of adequate power as well as proportion of the phase front for a system with minimal crosstalk. Here we study the design considerations for an OAM-multiplexed free-space data link, analyzing the power loss, channel crosstalk, and power penalty of the link in the case of limited-size receiver apertures and misalignment between the transmitter and the receiver. We describe the trade-offs for different transmitted beam sizes, receiver aperture sizes, and mode spacing of the transmitted OAM beams under given lateral displacements or receiver angular errors. Through simulations and some experiments, we show that (1) a system with a larger transmitted beam size and a larger receiver aperture is more tolerant to lateral displacement but less tolerant to the receiver angular error, and (2) a system with a larger mode spacing, which uses larger OAM charges, suffers more system power loss but less channel crosstalk; thus, a system with a small mode spacing shows a lower system power penalty when system power loss dominates (e.g., a small lateral displacement or receiver angular error), whereas that with a larger mode spacing shows a lower power penalty when channel crosstalk dominates (e.g., a larger lateral displacement or receiver angular error). This work could be beneficial to the practical implementation of OAM-multiplexed FSO links.

OCIS codes: (060.4230) Multiplexing; (060.4510) Optical communications; (060.2605) Free-space optical communication.

http://dx.doi.org/10.1364/OPTICA.2.000357

1. INTRODUCTION

Free-space optical (FSO) communication links can potentially benefit from the simultaneous transmission of multiple spatially orthogonal beams through a single aperture pair, such that each beam carries an independent data stream and the total capacity is multiplied by the number of beams [1–6]. Orthogonality of the beams enables efficient multiplexing and de-multiplexing at the transmitter and receiver, respectively. The use of orbital angular momentum (OAM) beams as an orthogonal modal basis set for multiplexing has received recent interest [3,5,6]. We note that there are other orthogonal modal basis sets, such as Hermite–Gaussian modes [7], that could be used for multiplexing data channels in free space. Although it is not straightforward to say which of these approaches is necessarily "better," OAM modes do offer the potential advantage of being conveniently matched to many optical subsystems due to their circular symmetry. Previous experimental reports [3] have included the demonstration of Tbit/s FSO data transmission using OAM multiplexing with a link distance of ~1 m. On the other hand, recent experiments have shown the feasibility of OAM beam transmission over distances of several kilometers [8]. Given the unique properties of OAM beams coupled with the recent scientific interest and the as-yet undetermined practical usefulness of OAM transmission, this paper is intended to help assess the potential viability and technical challenges of using multiple OAM modes for enhancing free-space communications over nontrivial distances.

With OAM, each beam has a phase front that "twists" in a helical fashion, and the beam's OAM order determines the

number of 2π phase shifts across the beam [9]. Such OAM beams have a ring-shaped intensity distribution and phase front of $\exp(i\ell\phi)$, where ℓ is the topological charge and ϕ is the azimuthal angle. Important characteristics of each OAM beam include the following: (i) intensity has a "doughnut" shape with little power in the center and (ii) the diameter of the beam grows with larger OAM order. Moreover, the amount of phase change per unit area is greatest in the center of the beam, and phase distribution is critical for ensuring modal purity and beam orthogonality.

For a practical system, the above characteristics of an OAM beam present several important challenges when designing an FSO communication link, such as (i) sufficient signal power and phase change needs to be recovered [10], and (ii) intermodal crosstalk should be minimized [11–14]. An important goal that has not been adequately explored in depth is to find the system limitations, trade-offs, and design parameters for an OAM-multiplexed FSO communication link.

In this paper, we explore the performance metrics and design considerations for an FSO communication link using OAM multiplexing. The design issues for the transmitted beam size, receiver aperture size, and mode spacing are given through the investigation of the system power loss, channel crosstalk, and system power penalty. By analyzing the power loss of the desired OAM channel due to beam divergence under a given limited-size aperture, a design consideration for the transmitted beam size is proposed. Through studying the effects of misalignment between the transmitter and the receiver (a lateral displacement or receiver angular error) on the OAM channel crosstalk and system power penalty, proper aperture sizes and mode spacing of the transmitted OAM beams could be selected to reduce system performance degradation. Our simulations and some experiments indicate that (i) a system with a larger beam size and a larger receiver aperture shows better tolerance to lateral displacement, but is less tolerant to the receiver angular error, and (ii) the selection of mode spacing for such a system could be based on a trade-off between signal power loss and crosstalk. For instance, a system with small mode spacing shows a lower system power penalty under a small lateral displacement or receiver angular error, whereas larger mode spacing shows a lower power penalty when the lateral displacement or receiver angular error is large.

Mode-multiplexed communication systems using other orthogonal modal sets will also likely suffer from signal power loss and intermodal crosstalk in a relatively similar fashion as OAM modes but with different parameters governing the link; therefore, the methods in this paper can be modified and adapted to potentially be used to determine the performance of other mode-multiplexed systems.

2. SYSTEM MODEL

A. Concept and Simulation Model

Figure 1 shows a schematic of an FSO communication link using OAM multiplexing. The multiplexed OAM beams diverge when transmitted through free space. By careful choice of the transmitted beam size, OAM mode spacing, and receiver aperture size, the system power loss, channel crosstalk, and system power penalty could be reduced.

Our simulation model of an OAM-multiplexed FSO communication link is depicted in Fig. 2. Independent data streams are

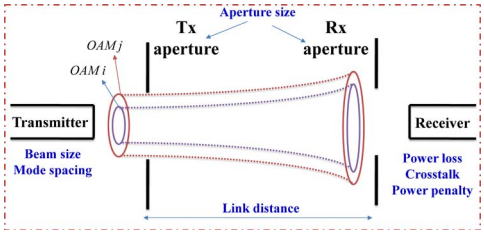

Fig. 1. Concept of an OAM-multiplexed FSO communication link.

carried by different collimated Gaussian beams at the same wavelength, each of which is coupled from a single-mode fiber to free space by a collimator. Each collimator is followed by a spiral phase plate (SPP) with a unique order to convert the Gaussian beam into a data-carrying OAM beam [15] [see Fig. 2(b)]. An SPP is defined by its thickness, which varies azimuthally according to

$$h(\phi) = \phi\ell\lambda/2\pi(n-1). \quad (1)$$

Its maximum thickness difference is $\Delta h = \ell\lambda/(n-1)$. Here, ϕ is the azimuthal angle varying from 0 to 2π, n is the refractive index of the plate material, and λ is the wavelength of the laser beam. Different orders of OAM beams are then multiplexed to form a concentric ring shape and are coaxially transmitted through free space. The multiplexed OAM beams are numerically propagated by using the Kirchhoff–Fresnel diffraction integral [16] to the receiver aperture located at a certain propagation distance. To investigate the signal power and crosstalk effects on neighboring OAM channels, the power distribution among the different OAM modes is analyzed through the modal decomposition approach, which corresponds to the case where the received OAM beams are de-multiplexed without power loss and the power of a desired OAM channel is completely collected by the receiver, which is infinitely large and perfectly aligned with the transmitter [12,14].

An experiment with a transmitted beam size of 2.2 mm over a 1 m link is carried out to partially validate our system model. In the experiment, spatial light modulators (SLMs), which cause spiral phase delays to the incoming beam by loading by a spiral phase hologram, are used to function as SPPs at the transmitter. At the receiver, the beams are de-multiplexed by another SLM loaded with an inverse spiral phase pattern of the desired mode to be detected and the resulting angularly flat phase front beam is then coupled into a single-mode fiber for power measurement.

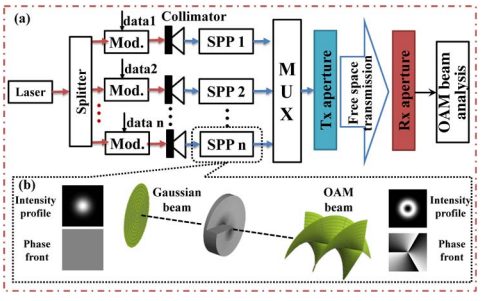

Fig. 2. (a) Simulation schematic of an OAM-multiplexed data link. (b) Conversion from a Gaussian beam into an OAM + 3 beam using an SPP + 3, which causes a helical phase shift from 0 to 6π. Mod., modulator; Tx, transmitter; Rx, receiver; SPP, spiral phase plate.

Assuming perfect fiber coupling, this process of OAM beam detection closely corresponds to the modal decomposition approach in our simulation model.

B. Assumptions

For convenience of analysis, the following assumptions are made:

- The wavelength of the laser source is 1550 nm. It should be noted that specific values in the analyzed results using other wavelengths might be different. However, our fundamental approach remains valid.
- All channels have the same transmitted power.
- The collimator output at the transmitter is assumed to be a fundamental Gaussian beam (i.e., OAM 0) and all OAM beams are generated from Gaussian beams with the same beam waist.
- The SPP at the transmitter is assumed to be "sufficiently large" to encompass the whole beam.
- The transmitter aperture is considered to be of the same size as the receiver aperture, which is reasonable in a bidirectional link. However, the transmitter aperture in our analysis is always larger than the transmitted beam size and we assume that it has no effect on the transmitted beam. Both the transmitter beam size and the receiver aperture size are parameters in the analysis.
- The insertion loss of the multiplexer is not considered, although it adds a constant insertion loss in a practical system. Besides, the insertion loss of the SPP, which is assumed to be independent of the OAM order, is also ignored.
- For calculations of spot size (beam diameter), the second moment of the intensity of an OAM beam or Gaussian beams, which is generally related to the beam waist, is employed, as given by the following equation:

$$D = 2\sqrt{\frac{2\int_0^{2\pi}\int_0^{\infty} r^2 I(r,\phi) r \mathrm{d}r\mathrm{d}\phi}{\int_0^{2\pi}\int_0^{\infty} I(r,\phi) r \mathrm{d}r\mathrm{d}\phi}}, \tag{2}$$

where $I(r,\phi)$ is the beam intensity profile and (r,ϕ) are polar coordinates [17].

- For the analysis of OAM carrying beams, we have considered Gaussian beams transformed into OAM beams by passing through SPPs (i.e., SPP-based OAM beams). Most of the OAM beams used in previously reported communication links are similar to the SPP-based OAM beams [3,18,19]. Although the OAM beams generated by passing Gaussian beams through SPPs are not exactly Laguerre–Gauss beams, such beams have similar characteristics in a communication link [20,21] (see Supplement 1 for further discussion).
- We only analyzed the case of a single-polarized system. Since there is no obvious crosstalk between different polarizations for the beam transmitted through free space, most of the results could also be applied to a dual-polarization system without further modifications [3,22].

C. Misalignments between the Transmitter and the Receiver

In an ideal case, the transmitter and the receiver would be perfectly aligned [i.e., the center of the receiver would overlap with the center of the transmitted beam, and the receiver would be perpendicular to the line connecting their centers, as shown in Fig. 3(a)]. However, in a practical system, due to jitter and vibration of the transmitter/receiver platform, the transmitter and the receiver may have lateral shifts relative to each other (i.e., lateral displacement) or may have angular shifts (i.e., receiver angular error), as depicted in Figs. 3(b) and 3(c), respectively [23]. Lateral displacement and receiver angular error might occur simultaneously. A specific example is a pointing error at the transmitter, which leads to both a lateral displacement and an angular error at the receiver, as depicted in Fig. 3(d).

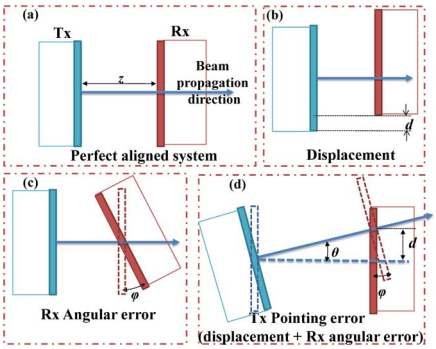

Fig. 3. Alignment between the transmitter and the receiver for (a) a perfectly aligned system, (b) a system with lateral displacement, (c) a system with a receiver angular error, and (d) a system with a transmitter pointing error. Tx, transmitter; Rx, receiver; z, transmission distance; d, lateral displacement; φ, receiver angular error; θ, pointing error.

Table 1. Parameters in the Model

D_t	Transmitted beam size (diameter)
D_a	Receiver aperture size (diameter)
z	Transmission distance of the link
d	Lateral displacement
φ	Receiver angular error
θ	Transmitter pointing error

In general, a practical link might use a tracking system to mitigate the random time-varying misalignment between the transmitter and the receiver due to system vibration or long-term drift. For example, there is a commercially available tracking system with lateral resolution below 0.1 mm and angular resolution below 1 μrad [24].

We analyze the performance of an FSO communication link by employing OAM multiplexing for the above scenarios. The parameters discussed are listed in Table 1.

3. SIGNAL POWER LOSS ANALYSIS

It is generally preferred to collect as much signal power as possible at the receiver in a communication link to ensure ample signal-to-noise ratio (SNR). Since OAM beams diverge while propagating in free space and available optical elements usually have limited aperture sizes due to component cost, it would be desirable to choose a proper transmitted beam size when designing an OAM-multiplexed FSO communication link over a certain transmission distance. In this section, we introduce approaches to design a suitable transmitted beam size by presenting our analyses of OAM beam divergence and power loss over different transmission distances due to limited-size apertures.

Given a fixed transmitted beam size, an OAM beam with a higher order has a larger spot size over a given distance. Figure 4(a) shows the divergence of different OAM beams when they have different transmitted beam sizes over a 100 m link.

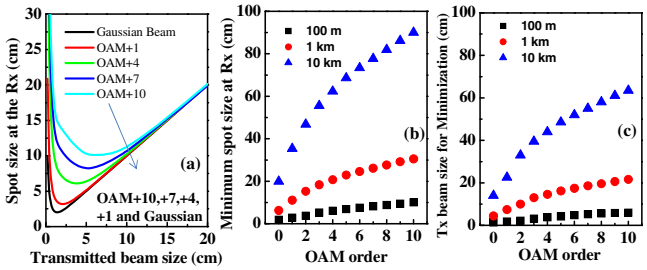

Fig. 4. (a) Simulated spot sizes (diameters) of different orders of OAM beams as a function of transmitted beam size given a link distance of 100 m. (b) Minimum spot sizes of different orders of OAM beams at different transmission link distances. (c) Relative transmitted beam size to achieve the minimum spot size at the receiver. Note that for the analysis of this figure only, the size of the receiver aperture is not considered.

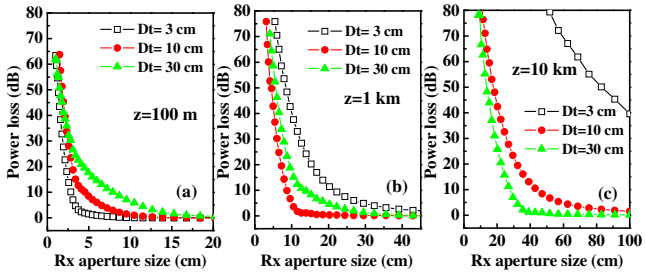

Fig. 5. Simulated power loss as a function of receiver aperture size (diameter) when only OAM + 3 is transmitted under perfect alignment for (a) $z = 100$ m, (b) $z = 1$ km, and (c) $z = 10$ km. D_t, transmitted beam size; z, transmission distance.

Take OAM + 4 as an example: when the transmitted beam size is less than 3 cm, the spot size at the receiver increases when increasing the transmitted beam size. This is because smaller beams diffract faster. However, when the transmitted beam size is larger than 3 cm, further increasing the transmitted beam leads to larger spot size at the receiver. This is because the geometrical characteristic of the beam dominates its diffraction characteristic. Such a trade-off needs to be considered to control the size of the received beam at a proper range when designing a link. For a specific transmission distance and OAM mode order, there exists a transmitted beam size to achieve a minimum spot size at the receiver. The minimum spot size at the receiver and the corresponding transmitted beam sizes for different link distances as a function of OAM mode order are shown in Figs. 4(b) and 4(c), respectively. These results indicate that (i) OAM beams with higher orders will have a larger minimum spot size given the same transmission distance, and (ii) the minimum spot size at the receiver grows approximately linearly with increase of the required transmitted beam size. For system design considerations, it is desirable to select parameters for the transmitted beam that ensure generally a minimum spot size at the receiver for all of the modes simultaneously. Here, we choose 3 and 10 cm as the transmitted beam sizes for the 100 m link, 10 and 30 cm for the 1 km link, and 30 cm for the 10 km link as examples for system performance analysis; although we did not include larger aperture sizes for the 10 km link simply due to the current state of practical sizes of the optical elements, we emphasize that our analysis can be extended to larger apertures and produce improved performance for longer distance systems.

One of the effects caused by a limited-size receiver aperture is signal power loss of the system, because the spot size of the diverged beam is too large to be fully captured. Figure 5 shows the power loss of OAM + 3 with different transmission distances and transmitted beam sizes. The power loss is directly related to the SNR of the received signal. We choose the receiver size to be 1.5 times the transmitted beam size; typically, this receiver size is large enough to capture sufficient power from the transmitted beam (e.g., in our case, less than 10 dB power loss for OAM + 3). If a free-space multimode OAM system has a common single receiver aperture for all modes, then higher-order OAM beams that diverge more during propagation have more power loss than lower-order OAM beams. Although we considered modes up to +10 for which the system penalties can be significant given the current state of practical aperture sizes, our analysis can be extended to higher-order modes.

4. CHANNEL CROSSTALK ANALYSIS

If the transmitter and the receiver are perfectly aligned (i.e., the received beam phase profile and the receiver aperture are concentric), then the power of the transmitted OAM mode does not spread into neighboring modes; this is due to the fact that orthogonality among different modes within a limited-size receiver aperture is still ensured based on recovering the full OAM phase change of the helical phase distribution [25]. However, in a practical system, the presence of a lateral displacement or a receiver angular error between the transmitter and the receiver causes a phase-profile mismatch between the incoming OAM beams and the receiver. This mismatch tends to reduce the received modal orthogonality, thereby leading to power leakage and crosstalk from the desired mode into adjacent modes.

A. Crosstalk Analysis for the System with Lateral Displacement

First, we investigate the effect of lateral displacement on channel crosstalk by fixing the receiver aperture size. Figure 6(a) shows the power distribution among different OAM modes due to a lateral displacement between the transmitter and the receiver when only OAM + 3 is transmitted. The transmitted beam size $D_t = 3$ cm and the receiver aperture size $D_a = 4.5$ cm. As the lateral

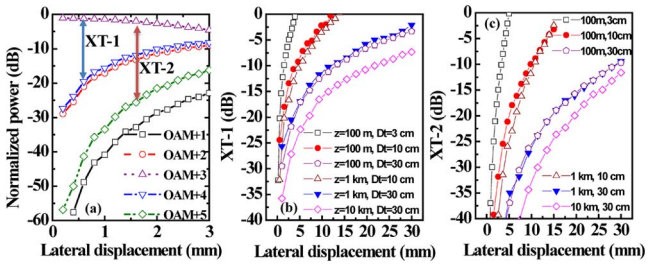

Fig. 6. (a) Simulated power distribution among different OAM modes as a function of lateral displacement over a 100 m link for which only the OAM + 3 mode is transmitted; the transmitted beam size $D_t = 3$ cm and the receiver aperture size D_a is 4.5 cm. (b, c) XT-1 and XT-2, respectively, as a function of lateral displacement for different transmission distances with different transmitted beam sizes. The receiver size is 1.5 times the transmitted beam size. XT-1, relative crosstalk to the nearest-neighboring mode (OAM + 4). XT-2, relative crosstalk to the second-nearest-neighboring mode (OAM + 5).

displacement increases, the power leaked into the other modes increases whereas the power on OAM + 3 decreases. This is because a larger displacement causes a larger mismatch between the received OAM beams and the receiver. The power leaked into OAM + 2 and OAM + 4 is greater than that of OAM + 1 and OAM + 5 due to their smaller mode spacing with respect to OAM + 3. One of the most important concerns is the power leaked into the nearest- and second-nearest-neighboring modes. Here we define the relative crosstalk to the nearest-neighboring mode XT-1 as the ratio of the power leaked into the nearest-neighboring mode (in our simulation, we examine OAM + 4) to the power on the desired mode (OAM + 3). Furthermore, XT-2 is defined as the relative crosstalk to the second-nearest-neighboring mode (OAM + 5 in our case). Figures 6(b) and 6(c) show the relative crosstalks XT-1 and XT-2, respectively, for different link distances with various transmitted beam sizes. The results indicate that (i) a larger transmitted beam size and longer transmission distances result in smaller XT-1 and XT-2, and (ii) a system with larger mode spacing is more tolerant to lateral displacement. Here, we use OAM + 3 as an example to analyze the power leakage into neighboring modes. However, it is expected that other modes would have similar performance trends.

B. Crosstalk Analysis for the System with a Receiver Angular Error

Besides lateral displacement, angular errors might also occur at the receiver. In the presence of a receiver angular error of magnitude φ, the incoming phase front hitting the receiver has an additional tilt-related term and its values on the edges of the beam form $\ell\phi \pm \varphi D/2$, where ℓ is the topological charge and ϕ is the azimuthal angle, and D is the spot size at the receiver. Clearly, these phase deviations from pure helicity are bound to introduce power leakage.

Figure 7(a) shows the power distribution among different OAM modes under different receiver angular errors when only OAM + 3 is transmitted with $D_t = 3$ cm and $D_a = 4.5$ cm. With a fixed receiver aperture size, a larger receiver angular error causes a higher power leakage into the other modes. Figures 7(b) and 7(c) show that the system with a larger transmitted beam size and a longer range has higher XT-1 and XT-2, respectively.

C. Specific Example of a Combination of Displacement and Receiver Angular Error: Transmitter Pointing Error

In a practical system, lateral displacement and receiver angular error might occur simultaneously, and the amounts of lateral displacement and receiver angular error might be random. Transmitter pointing error is an important parameter that determines the performance of a free-space OAM link. For our analysis, we consider transmitter pointing error to be a functional combination of both lateral displacement and receiver angular error. A transmitter pointing error of θ could be considered as a combination of a lateral displacement of $d = \tan(\theta) \times z$ and a receiver angular error of $\varphi = \theta$, where z is the link distance.

Figure 8(a) shows the power distribution among different OAM modes under different transmitter pointing errors when only OAM + 3 is transmitted with $D_t = 3$ cm and $D_a = 4.5$ cm. Given a fixed transmitter pointing error or receiver angular error, the power leakage in Fig. 8(a) is higher than that in Fig. 7(a) because a transmitter pointing error includes a lateral displacement in addition to the receiver angular error. Figures 8(b) and 8(c) show the XT-1 and XT-2, respectively, for a system with different transmission distances and transmitted beam sizes; we note that the trends of the results are similar to those shown in Figs. 7(b) and 7(c), respectively. This trend appears because the receiver angular error becomes the dominated factor that affects the system given a specific transmitter pointing error and transmitted beam size.

To reiterate the key points, a larger beam size at the receiver will result in two opposing effects: (i) a smaller lateral displacement-induced crosstalk because the differential phase change per unit area is smaller, and (ii) a larger tilt phase error-induced crosstalk because the phase error scales with a larger optical path delay.

5. POWER PENALTY ANALYSIS

Effects that are critical to determining proper system performance and design criteria include the power loss due to beam divergence and the channel crosstalk due to both lateral displacement and angular error. A consequence of signal power loss and channel crosstalk analyzed in the previous sections is an increase in system power penalty, which is the SNR difference needed to achieve a

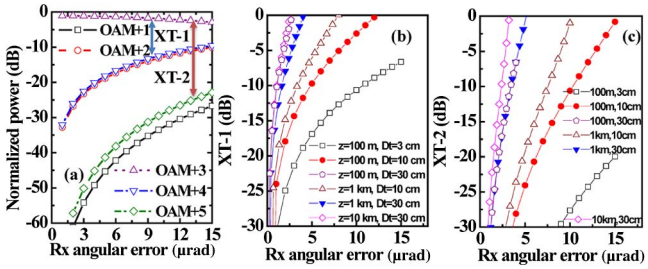

Fig. 7. (a) Simulated power distribution among different OAM modes as a function of receiver angular error over a 100 m link for which only the OAM + 3 is transmitted; the transmitted beam size D_t is 3 cm and the receiver aperture size D_a is 4.5 cm. (b, c) XT-1 and XT-2, respectively, as a function of receiver angular error for different transmission distances and transmitted beam sizes. The receiver size is 1.5 times the transmitted beam size. XT-1, relative crosstalk to the nearest-neighboring mode (OAM + 4). XT-2, relative crosstalk to the second-nearest-neighboring mode (OAM + 5).

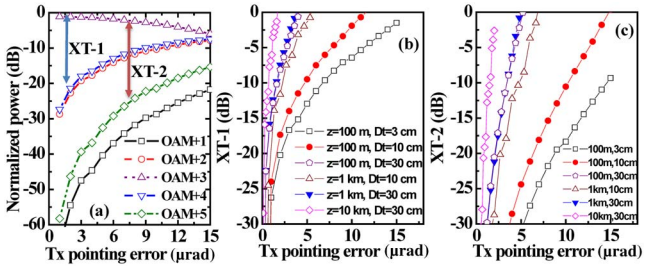

Fig. 8. (a) Simulated power distribution among different OAM modes as a function of transmitter pointing error over a 100 m link for which only OAM + 3 is transmitted; the transmitted beam size D_t is 3 cm and the receiver aperture size D_a is 4.5 cm. (b, c) XT-1 and XT-2, respectively, as a function of transmitter pointing error for different transmission distances and transmitted beam sizes. The receiver size is 1.5 times the transmitted beam size. XT-1, relative crosstalk to the nearest-neighboring mode (OAM + 4). XT-2, relative crosstalk to the second-nearest-neighboring mode (OAM + 5).

certain bit error rate (BER) by an OAM channel and an ideal channel. It is used as a metric to evaluate the system performance degradation. Signal power loss resulting from limited-size receiver apertures and channel crosstalk due to lateral displacement or receiver angular error degrade the signal-to-interference-plus-noise ratio of each channel, thus affecting the BER or power penalty performance. We simulated a four-channel OAM FSO communication link, with each channel transmitting a 16-QAM signal.

With the background noise assumed to follow the Gaussian model, the error probability of a 16-QAM signal is [26]

$$P_{e,16\text{-QAM}} = 3Q\left(\sqrt{\frac{4}{5}\frac{E_{\text{avg}}}{N_0}}\right)\left[1-\frac{3}{4}Q\left(\sqrt{\frac{4}{5}\frac{E_{\text{avg}}}{N_0}}\right)\right], \quad (3)$$

where E_{avg}/N_0 is the average SNR per bit. E_{avg} is the average signal power per bit and N_0 is the power density of Gaussian white noise, and $Q(\cdot)$ is the complementary error function [26]. Equation (3) allows the calculation of the minimum required transmitted power P_{rq} for a single channel (no crosstalk) to achieve a certain BER, given a Gaussian background noise N_0. In our simulation, we choose a forward error correction (FEC) limit of 3.8×10^{-3} as the BER threshold [27].

We assume that: (i) all channels have the same transmitted power; (ii) channel crosstalk interferes with the signal in a similar way as noise at our BER threshold [28]. Considering crosstalk effects in a mode-multiplexed system, the required transmitted power $P_{\text{rq},m}$ for channel m can be expressed as

$$P_{\text{rq},m} = P_{\text{rq}}\left(\alpha-\beta\cdot\frac{P_{\text{rq}}}{N_0}\right)^{-1}, \quad (4)$$

where α is the normalized signal power of the desired mode and β is the total crosstalk from all undesired modes. The power penalty is defined as

$$P_{\text{penalty}} = 10\cdot\log_{10}\left(\frac{P_{\text{rq},m}}{P_{\text{rq}}}\right)\text{dB}. \quad (5)$$

To explore the influence of limited-size receiver aperture and lateral displacement on power penalty, four channels are simulated in a 100 m OAM-multiplexed FSO communication link. A similar approach also applies to other link distances. Power penalties for all four channels might be different due to different OAM orders having different spots sizes. To ensure that every channel works, the largest power penalty among all channels is defined as the system power penalty.

We simulate various sets of OAM beams to analyze system power penalty with different mode spacing. Figure 9(a) shows the case of 3 cm transmitted beam size. When lateral displacement is larger than 0.75 mm, the system with mode spacing of 2 (OAM + 1, +3, +5, +7 transmitted) shows a lower power penalty than with mode spacing of 1 (OAM + 1, +2, +3, +4 transmitted). This is because the channel crosstalk between adjacent OAM modes is higher than that between the OAM modes with spacing of 2. When the lateral displacement is less than 0.75 mm, the system with mode spacing of 1 shows less power penalty than that with mode spacing of 2. This is because the system with mode spacing of 2 has a larger power loss due to the larger beam size at the receiver. Figure 9(b) shows the case when $D_t = 10$ cm and $D_a = 15$ cm. A comparison to the results in Fig. 9(a) shows that a larger transmitted beam size, which leads to a larger beam size at the receiver, could help reduce the system power penalty caused by lateral displacement.

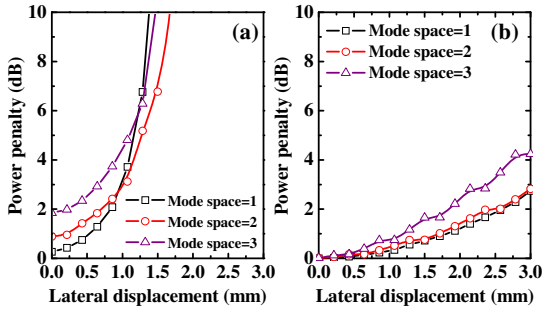

Fig. 9. Simulated system power penalty as a function of lateral displacement when different sets of OAM beams are transmitted over a 100 m link. Mode spacing = 1: OAM + 1, +2, +3, and +4 transmitted. Mode spacing = 2: OAM + 1, +3, +5, and +7 transmitted. Mode spacing = 3: OAM + 1, +4, +7, and +10 transmitted. (a) The transmitted beam size $D_t = 3$ cm and the receiver aperture size $D_a = 4.5$ cm. (b) $D_t = 10$ cm and $D_a = 15$ cm.

Similarly, the influence of receiver angular error on the system power penalty is also explored. Figure 10(a) shows the results when different sets of four OAM beams are transmitted over a 100 m link with $D_t = 3$ cm and $D_a = 4.5$ cm. Mode spacing of 2 has better performance than mode spacing of 1 when the receiver angular error is larger than 6 μrad. In Fig. 10(b), where $D_t = 10$ cm and $D_a = 15$ cm, the power penalty is slightly larger than that in Fig. 10(a). Figure 11 shows the system power penalty when there is a transmitter pointing error. Figure 11(a) shows a higher power penalty than does Fig. 10(a) because the transmitter pointing error contains extra lateral displacement besides the receiver angular error. In addition, Fig. 11(b) shows a trend similar to Fig. 10(b) because when the transmitted beam size and receiver aperture size are large, the power penalty is mostly caused by the receiver angular error rather than the lateral displacement.

The power penalty analysis indicates some selection rules for mode spacing: (i) a larger transmitted beam size and receiver aperture could increase the system tolerance to lateral displacement, but decrease its tolerance to receiver angular error, and (ii) systems with larger mode spacing have higher-order OAM beams, which leads to higher signal power loss due to beam divergence;

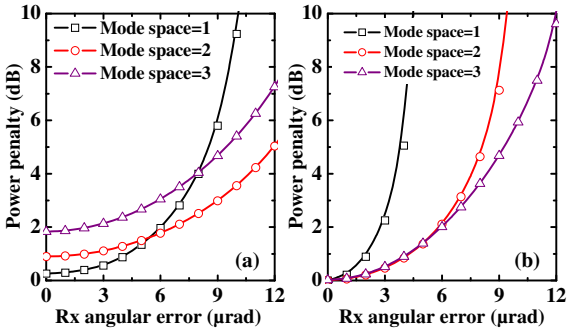

Fig. 10. Simulated system power penalty as a function of receiver angular error when different sets of OAM beams are transmitted in a 100 m link. (a) The transmitted beam size $D_t = 3$ cm and the receiver aperture size $D_a = 4.5$ cm. (b) $D_t = 10$ cm and $D_a = 15$ cm.

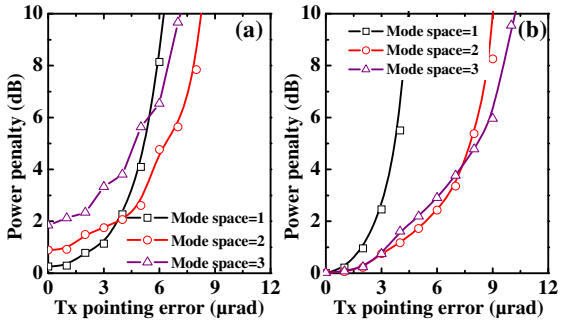

Fig. 11. Simulated system power penalty as a function of transmitter pointing error when different sets of OAM beams are transmitted in a 100 m link. (a) The transmitted beam size $D_t = 3$ cm and the receiver aperture size $D_a = 4.5$ cm. (b) $D_t = 10$ cm and $D_a = 15$ cm.

however, such systems also suffer less channel crosstalk. As a trade-off between signal power loss and crosstalk, a system with small mode spacing shows a lower system power penalty under a small lateral displacement or receiver angular error, whereas larger mode spacing shows a lower power penalty when the lateral displacement or receiver angular error is large.

6. SYSTEM PERFORMANCE IN THE PRESENCE OF BOTH LATERAL DISPLACEMENT AND RECEIVER ANGULAR ERROR

In a practical system, lateral displacement and receiver angular error might occur simultaneously. It has been shown in the previous section that when the transmitted beam size and receiver aperture size are larger, the system exhibits greater tolerance to lateral displacement but lower tolerance to angular error. Given certain lateral displacements and receiver angular errors, how to select the transmitted beam size and receiver aperture size to reduce the total power penalty would be an interesting question. In the section, we fix the mode spacing to two. Different transmitted beam sizes of 5, 6, 8, 10, and 15 cm with corresponding receiver aperture sizes of 7.5, 9, 12, 15, and 22.5 cm are considered.

Figure 12 shows the system power penalty for different transmitted beam sizes considering lateral displacement or receiver angular error. When the lateral displacement is 3 mm, a system with a transmitted beam size of 10 cm suffers ~6 dB less power penalty than that with a transmitted beam size of 6 cm [see Fig. 12(a)]. However, the former suffers 3 dB more power penalty than the latter when the receiver angular error is 10 μrad [see Fig. 12(b)]. There exists a trade-off between the effects of lateral displacement and receiver angular error. For the parameter design of a practical system, one might need to select a proper beam size to reduce the system performance degradation considering this trade-off.

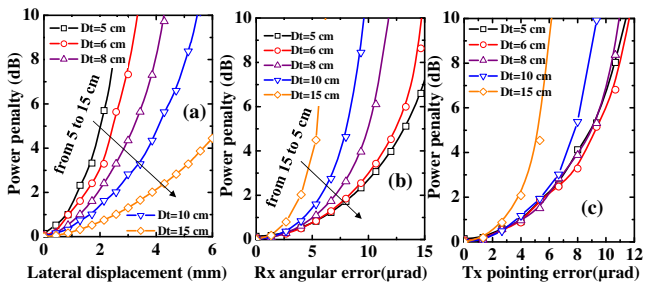

Fig. 12. Simulated system power penalty as a function of (a) lateral displacement, (b) receiver angular error, and (c) transmitter pointing error when mode spacing is 2 and transmission distance is 100 m. D_t, transmitted beam size. The receiver aperture size D_a is three times the transmitted beam size ($D_a = 1.5D_t$).

Figure 12(c) shows power penalty as a function of transmitter pointing error. A system with $D_t = 6$ cm shows the lowest power penalty than the others for different transmitting pointing errors. In terms of power penalty, a larger beam size at the receiver is more sensitive to the receiver angular error and less sensitive to lateral displacement. In addition, the effects of lateral displacement and receiver angular error are related to the transmitter pointing error and link distance. Therefore, for a given transmitter pointing error and link distance, trade-offs exist when considering different deleterious effects and choosing a beam size at the transmitter that minimizes the power penalty.

7. EXPERIMENTAL VALIDATION OF THE MODEL

As a partial validation of our link model, an experiment without misalignment between the transmitter and the receiver is first introduced. Figure 13(a) shows that the experimental results of the power loss of different OAM modes due to a limited-size receiver aperture are in good agreement with the simulation results.

Another validation of the simulation model considering a lateral displacement is shown in Fig. 13(b). Over the 1 m link and with a transmitted beam size of 2.2 mm, OAM + 3 is transmitted with a lateral displacement of 0.2 mm. Measured and simulated power distributions with different receiver apertures show similar trends.

8. ADDITIONAL CONSIDERATIONS

The following points are worth mentioning:

- We only consider the use of OAM beams with plus charges for data transmission. Our design approach could be similarly applied to systems in which OAM beams with both plus and minus charges are used for multiplexing [3,6,23].
- Atmospheric turbulence might result in beam distortions in an OAM-multiplexed FSO link [29–32]. Of all the effects caused by turbulence, beam wandering and arrival angle fluctuation

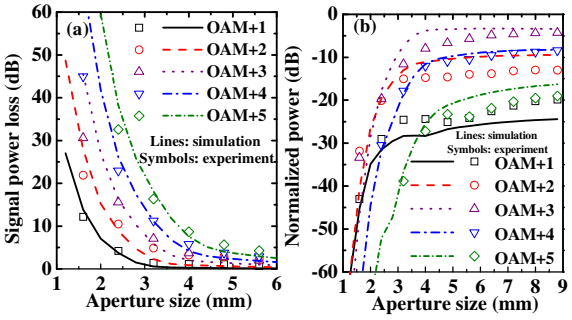

Fig. 13. (a) Comparison between the experimental and simulated power loss of different OAM beams as a function of receiver aperture size. The transmitter and receiver are perfectly aligned. (b) Comparison between experimental and simulated power distributions among different OAM modes as a function of receiver aperture size with a lateral displacement of 0.2 mm. Lines and symbols are simulation and experiment results, respectively.

could be considered as the lateral displacement and receiver angular error, respectively, discussed in our design approach. However, the intensity and phase fluctuation of the received beam caused by atmospheric turbulence might lead to severe signal fading at the receiver [30]. Such effects are not considered in our approach, but may need further exploration.

- Digital signal-processing algorithms, such as multiple input–multiple output equalization, which can be included in our simulations. The effects of lateral displacement and receiver angular error could be reduced if using such algorithms [33,34].
- In real-world systems, lateral displacement and receiver angular error are generally time-varying random processes that are typically described as beam jitter and beam wandering [30]. Our approach may help provide the analysis of the upper and lower bounds of system performance given a specific dynamic range of beam jitter and beam wandering.
- In a practical system, we might need to couple the beam into a receiving optics (e.g., a single-mode fiber) for signal detection. The angular error caused by beam deviation at the focal plane of such receiving optics has already been taken into account by mode decomposition.
- The link analysis and design criteria of this paper are provided for systems operating in the optical region of 1550 nm. We note that our general approach can also be applied to systems operating at other frequencies (e.g., millimeter wave [6,35,36]). Systems operating in other spectral ranges may have changes in dimensions as well as potential changes in performance trends.
- We focused on link distances of 100 m, 1 km, and 10 km. For a longer link distance, larger transmitter and receiver aperture sizes might be needed. For example, aperture size greater than 1 m might be needed for a link over several tens of kilometers.
- Our approach considered a system that uses collimated beams at the transmitter. However, there are beam-forming techniques at the transmitter that might prove beneficial for improved system performance [37].
- Although one can consider the tight alignment and aperture-size tolerances of the free-space OAM-multiplexed system to be technical challenges, one can also envision these added requirements as potentially providing an added benefit of increasing the difficulty of eavesdropping by any off-axis receivers.

9. SUMMARY

We have explored performance metrics and design parameters for OAM-multiplexed FSO communication links. The link distance, transmitted beam size, transmitter and receiver aperture sizes, and OAM mode spacing were studied holistically. By analyzing the system power loss, channel crosstalk, and system power penalty, a proper transmitted beam size, receiver aperture size, and OAM mode spacing could be selected for the system to handle lateral displacement, receiver angular error, or transmitter pointing error between the transmitter and the receiver.

Air Force Office of Scientific Research (AFOSR)(FA9550–15–C–0024); Defense Advanced Research Projects Agency (DARPA); Intel Labs University Research Office; National Science Foundation Major Research Instrumentation Program (NFS–MRI); NxGen Partners.

We thank Robert Boyd, Nivedita Chandrasekaran, Ivan Djordjevic, Michael Kendra, Prem Kumar, Mark Neifeld, David Ott, Miles Padgett, Soji Sajuyigbe, Jeffrey Shapiro, Shilpa Talwar, and Tommy Willis for fruitful discussions.

See Supplement 1 for supporting content.

REFERENCES

1. G. Gibson, J. Courtial, M. Padgett, M. Vasnetsov, V. Pas'ko, S. Barnett, and S. Franke-Arnold, "Free-space information transfer using light beams carrying orbital angular momentum," Opt. Express **12**, 5448–5456 (2004).
2. I. Djordjevic, "Deep-space and near-Earth optical communications by coded orbital angular momentum (OAM) modulation," Opt. Express **19**, 14277–14289 (2011).
3. J. Wang, J. Y. Yang, I. M. Fazal, N. Ahmed, Y. Yan, H. Huang, Y. Ren, Y. Yue, S. Dolinar, M. Tur, and A. E. Willner, "Terabit free-space data transmission employing orbital angular momentum multiplexing," Nat. Photonics **6**, 488–496 (2012).
4. A. Mair, A. Vaziri, G. Weihs, and A. Zeilinger, "Entanglement of the orbital angular momentum states of photons," Nature **412**, 313–316 (2001).
5. F. Tamburini, E. Mari, A. Sponselli, B. Thidé, A. Bianchini, and F. Romanato, "Encoding many channels on the same frequency through radio vorticity: first experimental test," New J. Phys. **14**, 1–17 (2012).
6. Y. Yan, G. Xie, M. P. Lavery, H. Huang, N. Ahmed, C. Bao, L. Li, Z. Zhao, A. F. Molisch, M. Tur, M. J. Padgett, and A. E. Willner, "High-capacity millimetre-wave communications with orbital angular momentum multiplexing," Nat. Commun. **5**, 4876 (2014).
7. S. Saghafi, C. Sheppard, and J. Piper, "Characterising elegant and standard Hermite–Gaussian beam modes," Opt. Commun. **191**, 173–179 (2001).
8. M. Krenn, R. Fickler, M. Fink, J. Handsteiner, M. Malik, T. Scheidl, R. Ursin, and A. Zeilinger, "Communication with spatially modulated light through turbulent air across Vienna," New J. Phys. **16**, 113028 (2014).
9. L. Allen, M. W. Beijersbergen, R. J. C. Spreeuw, and J. P. Woerdman, "Orbital angular momentum of light and the transformation of Laguerre–Gaussian laser modes," Phys. Rev. A **45**, 8185–8189 (1992).
10. H. J. Lezec, A. Degiron, E. Devaux, R. A. Linke, L. Martin-Moreno, F. J. Garcia-Vidal, and T. W. Ebbesen, "Beaming light from a subwavelength aperture," Science **297**, 820–822 (2002).
11. J. Anguita, M. Neifeld, and B. Vasic, "Turbulence-induced channel crosstalk in an orbital angular momentum-multiplexed free-space optical link," Appl. Opt. **47**, 2414–2429 (2008).
12. G. Xie, L. Li, Y. Ren, H. Huang, Y. Yan, N. Ahmed, Z. Zhao, M. P. J. Lavery, N. Ashrafi, S. Ashrafi, M. Tur, A. F. Molisch, and A. E. Willner, "Performance metrics and design parameters for an FSO communications link based on multiplexing of multiple orbital-angular-momentum beams," in *IEEE Globecom Workshop* (IEEE, 2014), pp. 481–486.
13. J. Torres, C. Osorio, and L. Torner, "Orbital angular momentum of entangled counter propagating photon," Opt. Lett. **29**, 1939–1941 (2004).
14. H. Qassim, F. M. Miatto, J. P. Torres, M. J. Padgett, E. Karimi, and R. W. Boyd, "Limitations to the determination of a Laguerre–Gauss spectrum via projective, phase-flattening measurement," J. Opt. Soc. Am. B **31**, A20–A23 (2014).
15. G. Turnbull, D. Robertson, and G. Smith, "The generation of free-space Laguerre–Gaussian modes at millimetre-wave frequencies by use of a spiral phase plate," Opt. Commun. **127**, 183–188 (1996).
16. R. Edgar, "The Fresnel diffraction images of periodic structures," J. Mod. Opt. **16**, 281–287 (1969).
17. R. Phillips and L. Andrews, "Spot size and divergence for Laguerre–Gaussian beams of any order," Appl. Opt. **22**, 643–644 (1983).
18. X. Cai, J. Wang, M. J. Strain, B. Johnson-Morris, J. Zhu, M. Sorel, J. L. O'Brien, M. G. Thompson, and S. Yu, "Integrated compact optical vortex beam emitters," Science **338**, 363–366 (2012).
19. T. Su, R. P. Scott, S. S. Djordjevic, N. K. Fontaine, D. J. Geisler, X. Cai, and S. J. B. Yoo, "Demonstration of free space coherent optical communication using integrated silicon photonic orbital angular momentum devices," Opt. Express **20**, 145–156 (2012).
20. N. Matsumoto, T. Ando, T. Inoue, Y. Ohtake, N. Fukuchi, and T. Hara, "Generation of high-quality higher-order Laguerre–Gaussian beams using liquid-crystal-on-silicon spatial light modulators," J. Opt. Soc. Am. A **25**, 1642–1651 (2008).
21. A. Yao and M. Padgett, "Orbital angular momentum: origins, behavior and applications," Adv. Opt. Photon. **3**, 161–204 (2011).

22. H. Huang, G. Xie, Y. Yan, N. Ahmed, Y. Ren, Y. Yue, D. Rogawski, M. J. Willner, B. I. Erkmen, K. M. Birnbaum, S. J. Dolinar, M. P. J. Lavery, M. J. Padgett, M. Tur, and A. E. Willner, "100 Tbit/s free-space data link enabled by three-dimensional multiplexing of orbital angular momentum, polarization, and wavelength," Opt. Lett. **39**, 197–200 (2014).
23. A. Farid and S. Hranilovic, "Outage capacity optimization for free space optical links with pointing errors," J. Lightwave Technol. **25**, 1702–1710 (2007).
24. http://photonic.ws/Free_Space_Optical_Communication_Tip-Tilt-Mirror_Brochure.pdf, 2014, pp. 6–7.
25. S. Franke-Arnold, S. M. Barnett, E. Yao, J. Leach, J. Courtial, and M. Padgett, "Uncertainty principle for angular position and angular momentum," New J. Phys. **6**, 103 (2004).
26. J. Proakis and M. Salehi, *Digital Communications*, 5th ed. (McGraw-Hill Higher Education, 2007).
27. International Telecommunication Union, "Forward error correction for high bit-rate DWDM submarine systems," ITU-T Recommendation G.975.1, Appendix I.9 (2004).
28. A. Molisch, *Wireless Communications*, 2nd ed. (Wiley, 2010).
29. X. Zhu and J. Kahn, "Free-space optical communication through atmospheric turbulence channels," IEEE Trans. Commun. **50**, 1293–1300 (2002).
30. L. Andrews and R. Phillips, *Laser Beam Propagation through Random Media* (SPIE, 2005).
31. N. Chandrasekaran and J. Shapiro, "Photon information efficient communication through atmospheric turbulence—part I: channel model and propagation statistics," J. Lightwave Technol. **32**, 1075–1087 (2014).
32. Y. Ren, H. Huang, G. Xie, N. Ahmed, Y. Yan, B. I. Erkmen, N. Chandrasekaran, M. P. J. Lavery, N. K. Steinhoff, M. Tur, S. Dolinar, M. Neifeld, M. J. Padgett, R. W. Boyd, J. H. Shapiro, and A. E. Willner, "Atmospheric turbulence effects on the performance of a free space optical link employing orbital angular momentum multiplexing," Opt. Lett. **38**, 4062–4065 (2013).
33. Q. Spencer, A. Swindlehurst, and M. Haardt, "Zero-forcing methods for downlink spatial multiplexing in multiuser MIMO channels," IEEE Trans. Signal Process. **52**, 461–471 (2004).
34. A. Goldsmith, S. A. Jafar, N. Jindal, and S. Vishwanath, "Capacity limits of MIMO channels," IEEE J. Sel. Areas Commun. **21**, 684–702 (2003).
35. B. Thidé, H. Then, J. Sjöholm, K. Palmer, J. Bergman, T. D. Carozzi, Y. N. Istomin, N. H. Ibragimov, and R. Khamitova, "Utilization of photon orbital angular momentum in the low-frequency radio domain," Phys. Rev. Lett. **99**, 087701 (2007).
36. M. Tamagnone, C. Craeye, and J. Perruisseau-Carrier, "Comment on 'Encoding many channels on the same frequency through radio vorticity: first experimental test'," New J. Phys. **14**, 118001 (2012).
37. L. Li, G. Xie, Y. Ren, N. Ahmed, H. Huang, Z. Zhao, P. Liao, M. P. J. Lavery, Y. Yan, C. Bao, Z. Wang, N. Ashrafi, S. Ashrafi, R. D. Linquist, M. Tur, and A. E. Willner, "Performance enhancement of an orbital angular momentum based free-space optical communication link through beam divergence controlling," in *Optical Fiber Communication* (Optical Society of America, 2015), paper M2F.6.